CHAPTER 1

Introduction

Chapter Outline

Models now in tanks we tow.
All of that to Froude we owe.
Will computers, fast and new,
Make us alter Euler's view?
Marshall Tulin

1.1. Overview of Problems and Approaches

The prediction of ship hydrodynamic performance can be broken down into the general areas of:

- resistance and propulsion;
- seakeeping and ship vibrations;
- maneuvring.

Propeller flows and propeller design can be seen as a subtopic of resistance and propulsion, but it is so important and features special techniques that it is treated as a separate topic in its own

Practical Ship Hydrodynamics. DOI: 10.1016/B978-0-08-097150-6.10001-6

right. Morgan and Lin (1998) give a good short introduction to the historical development of these techniques to the state of the art in the late 1990s.

The basic approaches can be roughly classified into:

- *Empirical/statistical approaches*. Design engineers need simple and reasonably accurate estimates, e.g. of the power requirements of a ship. Common approaches combine a rather simple physical model and regression analysis to determine required coefficients either from one parent ship or from a set of ships. The coefficients may be given in the form of constants, formulae, or curves. Because of the success with model testing, experimental series of hull forms have been developed for varying hull parameters. Extensive series were tested in the 1940s and the subsequent two decades. These series were created around a 'good' hull form as the parent form. The effect of essential hull parameters, e.g. block coefficient, was determined by systematic variations of these parameters. Because of the expense of model construction and testing, there are no recent comparable series tested of modern hull forms and the traditional ship series must be considered as outdated by now. Rather than using model tests, today computational fluid dynamics could be used to create data for systematic series varying certain parameters for a ship type (Harries and Tillig 2011). Once such a dedicated 'numerical hull series' is set up, designers can rapidly interpolate within such a database.
- *Experimental approaches, either in model tests or in full-scale trials*. The basic idea of model testing is to experiment with a scale model to extract information that can be scaled (transformed) to the full-scale ship. Despite continuing research and standardization efforts, a certain degree of empiricism is still necessary, particularly in the model-to-ship correlation, which is a method to enhance the prediction accuracy of ship resistance by empirical means. The total resistance can be decomposed in various ways. Traditionally, model basins tend to adopt approaches that seem most appropriate to their respective organization's corporate experience and accumulated databases. Unfortunately, this makes various approaches and related aggregated empirical data incompatible. Although there has been little change in the basic methodology of ship resistance since the days of Froude (1874), various aspects of the techniques have progressed. We now understand better the flow around three-dimensional, appended ships, especially the boundary layer effects. Also non-intrusive experimental techniques like laser-Doppler velocimetry (LDV) or particle image velocimetry (PIV) allow the measurement of the velocity field in the ship wake to improve propeller design. Another more recent experimental technique is wave pattern analysis to determine the wave-making resistance. In propulsion tests, measurements include towing speed and propeller quantities such as thrust, torque, and rpm. Normally, open-water tests on the propeller alone are run to aid the analysis process as certain coefficients are necessary for the propeller design. Strictly, open-water tests are not essential for power prediction. The model propeller is usually a stock propeller (taken from a large selection (= stock) of propellers) that approximates the actual design propeller.

Propulsion tests determine important input parameters for the actual detailed propeller design, e.g. wake fraction and thrust deduction. The wake distribution, also needed for propeller design, is measured behind the ship model using pitot tubes or laser-Doppler velocimetry (LDV). For propeller design, measured nominal wakes (for the ship without a propeller) for the model must be transformed to effective wakes (for the ship with a working propeller) for the full-scale ship. While semi-empirical methods for this transformation apparently work well for most hull forms, for those with considerable flow separation at the stern, i.e. typically full hulls, there are significant scale effects on the wake between model and full scale. To some extent, computational fluid dynamics can help here in estimating the scale effects. Although the procedures for predicting full-scale resistance from model tests are well accepted, full-scale data available for validation purposes are extremely limited and difficult to obtain. The powering performance of a ship is validated by actual ship trials, ideally conducted in calm seas. The parameters usually measured are torque, rpm, and speed. Thrust is measured only as a special requirement because of the difficulty and extra expense involved in obtaining accurate thrust data. Whenever possible and appropriate, corrections are made for the effects of waves, current, wind, and shallow water. Since the 1990s, the Global Positioning System (GPS) and computer-based data acquisition systems have considerably increased the accuracy and economy of full-scale trials. The GPS has eliminated the need for 'measured miles' trials near the shore with the possible contamination of data due to shallow-water effects. Today trials are usually conducted far away from the shore. Model tests for seakeeping are often used only for validation purposes. However, for open-top container ships and ro-ro ships model tests are often performed as part of the regular design process, as IMO regulations require certain investigations for ship safety which may be documented using model tests. Most large model basins have a maneuvring model basin. The favored method to determine the coefficients for the equations of motion is through a planar motion mechanism. However, scaling the model test results to full scale using the coefficients derived in this manner is problematic, because vortex shedding and flow separation are not similar between model and full scale. Appendages generally make scaling more difficult. Also, maneuvering tests have been carried out with radio-controlled models in lakes and large reservoirs. These tests introduce additional scale effects, since the model propeller operates in a different self-propulsion point than the full-scale ship propeller. Despite these concerns, the maneuvering characteristics of ships seem generally to be predicted with sufficient accuracy by experimental approaches.

- *Numerical approaches, either rather analytical or using computational fluid dynamics (CFD)*. For ship resistance and powering, CFD has become increasingly important and is now an indispensable part of the design process. Typically inviscid free-surface methods based on the boundary element approach are used to analyze the forebody, especially the interaction of bulbous bow and forward shoulder. Viscous flow codes focus on the aftbody or appendages. Flow codes modeling both viscosity and the wave-making are widely

applied for flows involving breaking waves. CFD is still considered by industry as too inaccurate for resistance or power predictions. So far CFD has been used to gain insight into local flow details and derive recommendation on how to improve a given design or select a most promising candidate design for model testing. However, numerical power prediction with good accuracy has been demonstrated in research applications by 2010 for realistic ship geometries. It is expected to drift into industry applications within the next decade. For seakeeping, simple strip methods are used to analyze the seakeeping properties. These usually employ boundary element methods to solve a succession of two-dimensional problems and integrate the results into a quasi-three-dimensional result with usually good accuracy. For water impact problems (slamming and sloshing), free-surface RANSE methods are widely used in industry practice. Also, for problems involving green water on deck, free-surface RANSE methods have become the preferred tool in practice, replacing previously favored non-linear boundary element methods. A commonly used method to predict the turning and steering of a ship is to use equations of motions with experimentally determined coefficients. Once these coefficients are determined for a specific ship design – by model tests, estimated from similar ships, by empirically enhanced strip methods or CFD – the equations of motions are used to simulate the dynamic behavior of the ship. The form of the equations of motions is fairly standard for most hull designs. The predictions can be used, for example, to select rudder size and steering control systems, or to predict the turning characteristics of ships. As viscous CFD codes became more robust and efficient to use, the reliance on experimentally derived coefficients in the equations of motions has been reduced. In some industry applications, CFD has been used exclusively to compute maneuvering coefficients for ship simulators, for example.

Although a model of the final ship design is still tested in a towing tank, the testing sequence and content have changed significantly over time. Traditionally, unless the new ship design was close to an experimental series or a known parent ship, the design process incorporated many model tests. The process has been one of design, test, redesign, test, etc., sometimes involving more than ten models, each with slight variations. This is no longer feasible due to time-to-market requirements from shipowners and no longer necessary thanks to CFD developments. Combining CAD (computer-aided design) to generate new hull shapes in concert with CFD to analyze these hull shapes allows for rapid design explorations without model testing. With massive parallel computing and progress in optimization strategies (e.g. response surfaces), formal optimization of hulls, propellers, and appendages has drifted into industrial applications. CFD is increasingly used for the actual design of hull and propellers. Then often only the final design is actually tested to validate the intended performance features and to get a power prediction accepted in practice as highly accurate. As a consequence of this practice, model tests for shipyard customers have declined considerably since the 1980s. This was partially compensated for by more sophisticated and detailed tests funded from research projects to validate and calibrate CFD methods.

One of the biggest problems for predicting ship seakeeping is determining the nature of the sea: how to predict and model it, for both experimental and computational analyses. Many long-term predictions of the sea require a Fourier decomposition of the sea and ship responses with an inherent assumption that the sea and the responses are 'moderately small', while the physics of many seakeeping problems is highly non-linear. Nevertheless, seakeeping predictions are often considered to be less important or covered by empirical safety factors where losses of ships are shrugged off as 'acts of God', until they occur so often or involve such spectacular losses of life that safety factors and other regulations are adjusted to a stricter level. Seakeeping is largely not understood by shipowners and global 'sea margins' of, e.g., 15% to finely tuned ($\pm 1\%$) power predictions irrespective of the individual design are not uncommon.

1.2. Model Tests – Similarity Laws

Since the purely numerical treatment of ship hydrodynamics has not yet reached a completely satisfactory stage, model tests are still essential in the design process and for validation purposes. The model tests must be performed such that model and full-scale ships exhibit similar behavior, i.e. the results for the model can be transferred to full scale by a proportionality factor. We indicate in the following the full-scale ship by the index s and the model by the index m.

We distinguish between:

- geometrical similarity;
- kinematical similarity;
- dynamical similarity.

Geometrical similarity means that the ratio of a full-scale 'length' (length, width, draft, etc.) L_s to a model-scale 'length' L_m is constant, namely the model scale λ:

$$L_s = \lambda \cdot L_m \tag{1.1}$$

Correspondingly we get for areas and volumes: $A_s = \lambda^2 \cdot A_m$; $\nabla_s = \lambda^3 \cdot \nabla_m$. In essence, the model then 'appears' to be the same as the full-scale ship. While this is essential for movie makers, it is not mandatory for naval architects who want to predict the hydrodynamic performance of a full-scale ship. In fact, there have been proposals to deviate from geometrical similarity to achieve better similarity in the hydrodynamics. However, these proposals were not accepted in practice and so we always strive at least in macroscopic dimensions for geometrical similarity. In microscopic dimensions, e.g. for surface roughness, geometrical similarity is not obtained.

Kinematic similarity means that the ratio of full-scale times t_s to model-scale times t_m is constant, namely the kinematic model scale τ:

$$t_s = \tau \cdot t_m \tag{1.2}$$

Geometrical and kinematical similarity result then in the following scale factors for velocities and accelerations:

$$V_s = \frac{\lambda}{\tau} \cdot V_m; \quad a_s = \frac{\lambda}{\tau^2} \cdot a_m \tag{1.3}$$

Dynamical similarity means that the ratio of all forces acting on the full-scale ship to the corresponding forces acting on the model is constant, namely the dynamical model scale:

$$F_s = \kappa \cdot F_m \tag{1.4}$$

Forces acting on the ship encompass inertial forces, gravity forces, and frictional forces.

Inertial forces follow Newton's law $F = m \cdot a$, where F denotes force, m mass, and a acceleration. For displacement ships, $m = \rho \cdot \nabla$, where ρ is the density of water and ∇ the displacement. We then obtain for ratio of the inertial forces:

$$\kappa = \frac{F_s}{F_m} = \frac{\rho_s}{\rho_m} \cdot \frac{\nabla_s}{\nabla_m} \cdot \frac{a_s}{a_m} = \frac{\rho_s}{\rho_m} \cdot \frac{\lambda^4}{\tau^2} \tag{1.5}$$

This equation couples all three scale factors. It is called Newton's law of similarity. We can rewrite Newton's law of similarity as:

$$\kappa = \frac{F_s}{F_m} = \frac{\rho_s}{\rho_m} \cdot \lambda^2 \cdot \left(\frac{\lambda}{\tau}\right)^2 = \frac{\rho_s}{\rho_m} \cdot \frac{A_s}{A_m} \cdot \left(\frac{V_s}{V_m}\right)^2 \tag{1.6}$$

Hydrodynamic forces are often described by a coefficient c as follows:

$$F = c \cdot \frac{1}{2} \rho \cdot V^2 \cdot A \tag{1.7}$$

V is a reference speed (e.g. ship speed), A a reference area (e.g. wetted surface in calm water). The factor ½ is introduced in analogy to stagnation pressure $q = ½\rho \cdot V^2$. Combining the above equations then yields:

$$\frac{F_s}{F_m} = \frac{c_s \cdot \frac{1}{2} \rho_s \cdot V_s^2 \cdot A_s}{c_m \cdot \frac{1}{2} \rho_m \cdot V_m^2 \cdot A_m} = \frac{\rho_s}{\rho_m} \cdot \frac{A_s}{A_m} \cdot \left(\frac{V_s}{V_m}\right)^2 \tag{1.8}$$

This results in $c_s = c_m$, i.e. the non-dimensional coefficient c is constant for both ship and model. For the same non-dimensional coefficients Newton's similarity law is fulfilled and vice versa.

Gravity forces can be described in a similar fashion as inertial forces:

$$G_s = \rho_s \cdot g \cdot \nabla_s \text{ resp. } G_m = \rho_m \cdot g \cdot \nabla_m \tag{1.9}$$

This yields another force scale factor:

$$\kappa_g = \frac{G_s}{G_m} = \frac{\rho_s}{\rho_m} \cdot \frac{\nabla_s}{\nabla_m} = \frac{\rho_s}{\rho_m} \cdot \lambda^3 \tag{1.10}$$

For dynamical similarity both force scale factors must be the same, i.e. $\kappa = \kappa_g$. This yields for the time scale factor:

$$\tau = \sqrt{\lambda} \tag{1.11}$$

We can now eliminate the time scale factors in all equations above and express the proportionality exclusively in the length scale factor λ, e.g.:

$$\frac{V_s}{V_m} = \sqrt{\lambda} \quad \rightarrow \quad \frac{V_s}{\sqrt{L_s}} = \frac{V_m}{\sqrt{L_m}} \tag{1.12}$$

It is customary to make the ratio of velocity and square root of length non-dimensional with $g = 9.81$ m/s^2. This yields the Froude number:

$$F_n = \frac{V}{\sqrt{g \cdot L}} \tag{1.13}$$

The same Froude number in model and full scale ensures dynamical similarity only if inertial and gravity forces are present (Froude's law). For the same Froude number, the wave pattern in model and full scale are geometrically similar. This is only true for waves of small amplitude where gravity is the only relevant physical mechanism. Breaking waves and splashes involve another physical mechanism (e.g. surface tension) and do not scale so easily. Froude's law is kept in all regular ship model tests (resistance and propulsion tests, seakeeping tests, maneuvering tests). This results in the following scales for speeds, forces, and powers:

$$\frac{V_s}{V_m} = \sqrt{\lambda} \qquad \frac{F_s}{F_m} = \frac{\rho_s}{\rho_m} \cdot \lambda^3 \qquad \frac{P_s}{P_m} = \frac{F_s \cdot V_s}{F_m \cdot V_m} = \frac{\rho_s}{\rho_m} \cdot \lambda^{3.5} \tag{1.14}$$

Frictional forces follow yet another similarity law, and are primarily due to frictional stresses (due to friction between two layers of fluid):

$$R = \mu \cdot \frac{\partial u}{\partial n} \cdot A \tag{1.15}$$

μ is a material constant, namely the dynamic viscosity. The partial derivative is the velocity gradient normal to the flow direction. A is the area subject to the frictional stresses. Then the ratio of the frictional forces is:

$$\kappa_f = \frac{R_s}{R_m} = \frac{\mu_s (\partial u_s / \partial n_s) A_s}{\mu_m (\partial u_m / \partial n_m) A_m} = \frac{\mu_s}{\mu_m} \cdot \frac{\lambda^2}{\tau} \tag{1.16}$$

Again we demand that the ratio of frictional forces and inertial forces should be the same, $\kappa_f = \kappa$. This yields:

$$\frac{\mu_s}{\mu_m} \cdot \frac{\lambda^2}{\tau} = \frac{\rho_s}{\rho_m} \cdot \frac{\lambda^4}{\tau^2} \tag{1.17}$$

If we introduce the kinematic viscosity $\nu = \mu/\rho$ this yields:

$$\frac{\nu_s}{\nu_m} = \frac{\lambda^2}{\tau} = \frac{V_s \cdot L_s}{V_m \cdot L_m} \quad \rightarrow \quad \frac{V_s \cdot L_s}{\nu_s} = \frac{V_m \cdot L_m}{\nu_m} \tag{1.18}$$

$R_n = V \cdot L/\nu$ is the Reynolds number, a non-dimensional speed parameter important in viscous flows. The same Reynolds number in model and full scale ensures dynamic similarity if only inertial and frictional forces are present (Reynolds' law). (This is somewhat simplified as viscous flows are complicated by transitions from laminar to turbulent flows, microscopic-scale effects such as surface roughness, flow separation, etc.) The kinematic viscosity ν of seawater [m/s^2] can be estimated as a function of temperature t (°C) and salinity s (%):

$$\nu = 10^{-6} \cdot (0.014 \cdot s + (0.000645 \cdot t - 0.0503) \cdot t + 1.75) \tag{1.19}$$

Sometimes slightly different values for the kinematic viscosity of water may be found. The reason is that water is not perfectly pure, containing small organic and inorganic matter which differs regionally and in time.

Froude number and Reynolds number are related by:

$$\frac{R_n}{F_n} = \frac{V \cdot L}{\nu} \cdot \frac{\sqrt{gL}}{V} = \frac{\sqrt{gL^3}}{\nu} \tag{1.20}$$

Froude similarity is easy to fulfill in model tests, as with smaller models also the necessary test speed decreases. Reynolds' law on the other hand is difficult to fulfill as smaller models mean higher speeds for constant kinematic viscosity. Also, forces do not scale down for constant viscosity.

Ships operating at the free surface are subject to gravity forces (waves) and frictional forces. Thus in model tests both Froude's and Reynolds' laws should be fulfilled. This would require:

$$\frac{R_{ns}}{R_{nm}} = \frac{\nu_m}{\nu_s} \cdot \sqrt{\frac{L_s^3}{L_m^3}} = \frac{\nu_m}{\nu_s} \cdot \lambda^{1.5} = 1 \tag{1.21}$$

i.e. model tests should chose model scale and viscosity ratio of the test fluid such that $(\nu_m/\nu_s) \cdot \lambda^{1.5} = 1$ is fulfilled. Such fluids do not exist or at least are not cheap and easy to handle

for usual model scales. However, sometimes the test water is heated to improve the viscosity ratio and reduce the scaling errors for viscous effects.

Söding (1994) proposed 'sauna tanks' where the water is heated to a temperature of 90°C. Then the same Reynolds number as in cold water can be reached using models of only half the length. Smaller tanks could be used which could be better insulated and may actually require less energy than today's large tanks. The high temperature would also allow similar cavitation numbers as for the full-scale ship. A futuristic towing tank may be envisioned that would also perform cavitation tests on propellers, eliminating the need for special cavitation tunnels. However, such 'sauna tanks' have not been established yet and there are doubts concerning the feasibility of such a concept.

For model tests investigating vibrations Froude's similarity law does not automatically also give *similarity in vibrations*. For example, for propeller blade vibrations, model propellers of the same material as the full-scale propeller are too stiff under Froude similarity. Similarity in vibrations follows Cauchy's scaling law, requiring that the Cauchy number is the same in model and full scale:

$$C_n = \frac{E \cdot I \cdot t^2}{\rho \cdot g \cdot L^6} \tag{1.22}$$

where E is the modulus of elasticity, I the moment of inertia, t the time, and L the length. The same Cauchy and Froude numbers mean that, for the same density, the modulus of elasticity is downscaled by λ from full scale to model scale.

1.3. Full-Scale Trials

Trial tests of the built ship are an important prerequisite for the acceptance of the ship by the shipowner and are always specified in the contract between shipowner and shipyard. The problem is that the trial conditions differ from both model test conditions and design conditions. The contract usually specifies a contract speed at design load at a given percentage of the maximum continuous rating of the engine, this at calm sea without wind and current on deep water. Trial conditions are usually in ballast load, natural seaways, in the presence of currents and sometimes shallow water. Only on rare occasions is it possible to perform trial tests under ideal conditions as specified in the contract. However, upper limits for the wind and sea conditions are usually defined in the contract and test trials are performed only at times or places where the actual conditions are within the specified limits.

The difference between contract and trial conditions requires various corrections to correlate trial results to contract conditions. Apart from the difficulties and margins of uncertainties in

the trial measurements, the correlation procedure is plagued by many doubts. The traditional methods are partly empirical, involving curves with manual interpolation, etc. It was not uncommon that the results of various consultants, e.g. towing tank experts, differed by several tenths of a knot for the obtainable speed under contract conditions. This margin may make a difference between paying and not paying considerable penalties! Subsequently, trial evaluation was susceptible to disputes between representatives of shipowners and shipyards. The increasing demand for quality management and clearly documented procedures, preferably on an international standard, led to the formation of various panels of experts. The Japan Marine Standards Association submitted in 1998 a proposal for an ISO standard for the assessment of speed and power in speed trials. Also, the 'trial and monitoring' subcommittee of the ITTC (International Towing Tank Conference) was tasked with the development of an international standard.

Test trials were historically 'measured mile trials', as ships were tested between measured miles near the coast for different ship speeds. The ship speed can be measured 'over ground' (relative to the earth) or 'in water' (relative to the water). The speed in water includes currents and local flow changes. Historically, various logs have been developed, including devices towed behind the ship, on long rods alongside the ship, electro-acoustic devices, and pitot tubes in the ship bottom. There is still no accurate and reliable way to measure a ship's speed through water. The speed over ground was traditionally determined by electro-acoustic devices, celestial navigation, and radio navigation. The advent of satellite systems, namely GPS (global positioning system) and DGPS (differential GPS), has eliminated many of the previous uncertainties and problems. GPS allows accurate determination of the speed over ground, although the speed of interest is the speed in water. Trials are usually performed by repeatedly testing the ship on opposite courses to eliminate the effects of current. It is best to align the course with the wind and predominant wave propagation direction to make elimination of these effects in the correlation procedure easier.

Seakeeping is usually not measured in detail as a normal procedure in ship deliveries. Full-scale seakeeping tests are sometimes used in research and are discussed in more detail in Section 4.2.

1.4. Numerical Approaches (Computational Fluid Dynamics)

1.4.1. Basic Equations

For the velocities involved in ship flows, water can be regarded as incompressible, i.e. the density ρ is constant. Therefore we will limit ourselves here to incompressible flows. All equations are given in a Cartesian coordinate system with z pointing downwards.

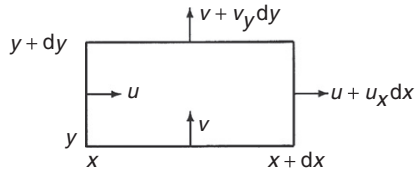

Figure 1.1:
Control volume to derive continuity equation in two dimensions

The continuity equation states that any amount flowing into a control volume also flows out of the control volume at the same time. We consider for the two-dimensional case an infinitely small control volume as depicted in Fig. 1.1. u and v are the velocity components in x resp. y direction. The indices denote partial derivatives, e.g. $u_x = \partial u/\partial x$. Positive mass flux leaves the control volume; negative mass flux enters the control volume. The total mass flux has to fulfill:

$$-\rho\, \mathrm{d}y\, u + \rho\, \mathrm{d}y\, (u + u_x\, \mathrm{d}x) - \rho\, \mathrm{d}x\, v + \rho\, \mathrm{d}x\, v + \rho\, \mathrm{d}x\, (v + v_y\, \mathrm{d}y) = 0 \tag{1.23}$$

$$u_x + v_y = 0 \tag{1.24}$$

The continuity equation in three dimensions can be derived correspondingly to:

$$u_x + v_y + w_z = 0 \tag{1.25}$$

where w is the velocity component in z direction.

The Navier–Stokes equations together with the continuity equation suffice to describe all real flow physics for ship flows. The Navier–Stokes equations describe conservation of momentum in the flow:

$$\begin{aligned}
\rho(u_t + uu_x + vu_y + wu_z) &= \rho f_1 - p_x + \mu(u_{xx} + u_{yy} + u_{zz}) \\
\rho(v_t + uv_x + vv_y + wv_z) &= \rho f_2 - p_y + \mu(v_{xx} + v_{yy} + v_{zz}) \\
\rho(w_t + uw_x + vw_y + ww_z) &= \rho f_3 - p_z + \mu(w_{xx} + w_{yy} + w_{zz})
\end{aligned} \tag{1.26}$$

where f_i is an acceleration due to a volumetric force, p the pressure, μ the viscosity, and t the time. Often the volumetric forces are neglected, but gravity can be included by setting $f_3 = g$ ($= 9.81\ \mathrm{m/s^2}$) or the propeller action can be modeled by a distribution of volumetric forces f_1. The l.h.s. of the Navier–Stokes equations without the time derivative describes convection, the time derivative describes the rate of change ('source term'), the last term on the r.h.s. describes diffusion.

The Navier–Stokes equations in the above form contain on the l.h.s. products of the velocities and their derivatives. This is a non-conservative formulation of the Navier–Stokes equations. A conservative formulation contains unknown functions (here velocities) only as first derivatives. Using the product rule for differentiation and the continuity equation, the

non-conservative formulation can be transformed into a conservative formulation, e.g. for the first of the Navier–Stokes equations above:

$$\begin{aligned}(u^2)_x + (uv)_y + (uw)_z &= 2uu_x + u_y v + uv_y + u_z w + uw_z \\ &= uu_x + vu_y + wu_z + u\underbrace{(u_x + v_y + w_z)}_{=0} \\ &= uu_x + vu_y + wu_z\end{aligned} \tag{1.27}$$

Navier–Stokes equations and the continuity equation form a system of coupled, non-linear partial differential equations. An analytical solution of this system is impossible for ship flows. Even if the influence of the free surface (waves) is neglected, today's computers are not powerful enough to allow a numerical solution either. Even if such a solution may become feasible in the future, it is questionable if it is really necessary for engineering purposes in naval architecture.

Velocities and pressure may be divided into a time average and a fluctuation part to bring the Navier–Stokes equations closer to a form where a numerical solution is possible. Time averaging yields the Reynolds-averaged Navier–Stokes equations (RANSE). u, v, w, and p are from now on time averages. u', v', w' denote the fluctuation parts. For unsteady flows (e.g. maneuvering), high-frequency fluctuations are averaged over a chosen time interval (assembly average). This time interval is small compared to the global motions, but large compared to the turbulent fluctuations. Most computations for ship flows are limited to steady flows where the terms u_t, v_t, and w_t vanish. The RANSE have a similar form to the Navier–Stokes equations:

$$\begin{aligned}\rho(u_t + uu_x + vu_y + wu_z) &= \rho f_1 - p_x + \mu(u_{xx} + u_{yy} + u_{zz}) \\ &\quad -\rho((\overline{u'u'})_x + (\overline{u'v'})_y + (\overline{u'w'})_z) \\ \rho(v_t + uv_x + vv_y + wv_z) &= \rho f_2 - p_y + \mu(v_{xx} + v_{yy} + v_{zz}) \\ &\quad -\rho((\overline{u'v'})_x + (\overline{v'v'})_y + (\overline{v'w'})_z) \\ \rho(w_t + uw_x + vw_y + ww_z) &= \rho f_3 - p_z + \mu(w_{xx} + w_{yy} + w_{zz}) \\ &\quad -\rho((\overline{u'w'})_x + (\overline{v'w'})_y + (\overline{w'w'})_z)\end{aligned} \tag{1.28}$$

They contain as additional terms the derivatives of the Reynolds stresses:

$$\begin{aligned}&-\rho\overline{u'u'} - \rho\overline{u'v'} - \rho\overline{u'w'} \\ &-\rho\overline{u'v'} - \rho\overline{v'v'} - \rho\overline{v'w'} \\ &-\rho\overline{u'w'} - \rho\overline{v'w'} - \rho\overline{w'w'}\end{aligned} \tag{1.29}$$

The time averaging eliminated the turbulent fluctuations in all terms except the Reynolds stresses. The RANSE require a turbulence model that couples the Reynolds stresses to the

average velocities. There are whole books and conferences dedicated to turbulence modeling. Recommended for further studies is, e.g., Ferziger and Peric (1996). Turbulence modeling will not be treated in detail here, except for a brief discourse in Section 1.5.1. It suffices to say that, despite considerable progress in turbulence modeling, none of the present models is universally convincing and research continues to look for better solutions for ship flows. Because we are so far from being able to solve the actual Navier−Stokes equations, we often say 'Navier−Stokes' (as in Navier−Stokes solver) when we really mean RANSE.

'Large-eddy simulations' (LES) are located between Navier−Stokes equations and RANSE. LES let the grid resolve the large vortices in the turbulence directly and only model the smaller turbulence structures. Depending on what is considered 'small', this method lies closer to RANSE or actual Navier−Stokes equations. So far few researchers have attempted LES computations for ship flows and the grid resolution was often too coarse to allow any real progress compared to RANSE solutions. However, many experts see LES as a key technology for maritime CFD applications that may drift into industry application within the next two decades.

Neglecting viscosity − and thus of course all turbulence effects − turns the Navier−Stokes equations (also RANSE) into the Euler equations, which still have to be solved together with the continuity equations:

$$\begin{aligned} \rho(u_t + uu_x + vu_y + wu_z) &= \rho f_1 - p_x \\ \rho(v_t + uv_x + vv_y + wv_z) &= \rho f_2 - p_y \\ \rho(w_t + uw_x + vw_y + ww_z) &= \rho f_3 - p_z \end{aligned} \tag{1.30}$$

Euler solvers allow coarser grids and are numerically more robust than RANSE solvers. They are suited for computation of flows about lifting surfaces (foils) and are thus popular in aerospace applications. They are not so well suited for ship flows and generally not recommended because they combine the disadvantages of RANSE and Laplace solvers without being able to realize their major advantages: programming is almost as complicated as for RANSE solvers, but the physical model offers hardly any improvements over simple potential flow codes (Laplace solvers).

A further simplification is the assumption of irrotational flow:

$$\nabla \times \vec{v} = \begin{Bmatrix} \partial/\partial x \\ \partial/\partial y \\ \partial/\partial z \end{Bmatrix} \times \vec{v} = 0 \tag{1.31}$$

A flow that is irrotational, inviscid and incompressible is called potential flow. In potential flows the components of the velocity vector are no longer independent from each other. They

are coupled by the potential ϕ. The derivative of the potential in arbitrary direction gives the velocity component in this direction:

$$\vec{v} = \begin{Bmatrix} u \\ v \\ w \end{Bmatrix} = \nabla\phi \tag{1.32}$$

Three unknowns (the velocity components) are thus reduced to one unknown (the potential). This leads to a considerable simplification of the computation.

The continuity equation simplifies to Laplace's equation for potential flow:

$$\Delta\phi = \phi_{xx} + \phi_{yy} + \phi_{zz} = 0 \tag{1.33}$$

If the volumetric forces are limited to gravity forces, the Euler equations can be written as:

$$\nabla\left(\phi_t + \frac{1}{2}(\nabla\phi)^2 - gz + \frac{1}{\rho}p\right) = 0 \tag{1.34}$$

Integration gives Bernoulli's equation:

$$\phi_t + \frac{1}{2}(\nabla\phi)^2 - gz + \frac{1}{\rho}p = \text{const.} \tag{1.35}$$

The Laplace equation is sufficient to solve for the unknown velocities. The Laplace equation is linear. This offers the big advantage of combining elementary solutions (so-called sources, sinks, dipoles, vortices) to arbitrarily complex solutions. Potential flow codes are still the most commonly used CFD tools in ship and propeller design.

Boundary layer equations represent a special branch in the development of hydrodynamics (see Schlichting 1979), which are historically important. The boundary layer equations introduce many simplifications in the physical model: diffusion in the predominant flow direction is neglected, the thickness of the boundary layer is taken as small, and the pressure is constant over the thickness. These assumptions are violated near separating boundary layers. Therefore separation cannot be predicted properly. Of course, neither is any evaluation of the separated flow possible. But this is the area of interest for improving aftbodies and designing the propeller. One of the last doctoral theses on boundary layer methods for ship flows concluded in 1993: 'With the present method the practically interesting velocities at the propeller plane cannot be determined because there is no wall. In order to compute all the velocity components in a thick boundary layer and at the propeller plane, the Navier−Stokes equations have to be solved.'

Boundary layer methods had been substituted almost completely by RANSE solvers by the end of the 1980s. A series of validation workshops demonstrated that the solution of the equations for thin boundary layers failed in the stern region because of the rapid thickening of the

boundary layer in this zone. The limited success of generalizations of thin boundary layer equations involving high-order corrections was subsequently demonstrated so that the tendency towards computing the full solution of the Navier–Stokes equations became stronger and stronger because increased computer resources became more and more available at continuously decreasing costs.

Basic equations (and flows) are sometimes classified as elliptic, hyperbolic or parabolic. Consider a two-dimensional differential equation of second order:

$$A\frac{\partial^2 f}{\partial x^2} + 2B\frac{\partial^2 f}{\partial x \partial y} + C\frac{\partial^2 f}{\partial y^2} + a\frac{\partial f}{\partial x} + b\frac{\partial f}{\partial y} + cf + d = 0 \tag{1.36}$$

For $\delta = AC - B^2 > 0$ the equation is 'elliptic', for $\delta = 0$ 'parabolic' and for $\delta < 0$ 'hyperbolic'. The names are derived from an analogy to the algebraic equation:

$$Ax^2 + 2Bxy + Cy^2 + ax + by + d = 0 \tag{1.37}$$

This equation describes for $\delta > 0$ an ellipse, for $\delta = 0$ a parabola, and for $\delta < 0$ a hyperbola. Behind these rather abstract mathematical definitions lies a physical meaning (Fig. 1.2):

- *Elliptic.* disturbances propagate in all directions. RANSE and the Laplace equation are in general elliptic.
- *Hyperbolic.* Disturbances are limited in their propagation to a conical (or in two dimensions a wedge-shaped) region. Supersonic flow with a Mach cone follows a hyperbolic field equation. The Kelvin angle in the wave pattern results in a radiation condition of 'hyperbolic' character.
- *Parabolic.* The extreme case of a hyperbolic flow is a parabolic flow. Here the angle of the cone/wedge opens up to 90°. Disturbances propagate only downstream. 'Parabolic' RANSE solvers allow faster solution with reduced storage requirements. They start the computation at the upstream end and solve strip after strip marching downstream. Instead of considering the whole domain at one time, only two adjacent strips have to be considered at any time. However, local flow reversals could never be captured by such a method because they violate the assumed parabolic character of the flow. Parabolic RANSE solvers thus appeared only shortly in the 1980s and were replaced by fully elliptic solvers when more computer power became widely available. All unsteady equations are parabolic in time.

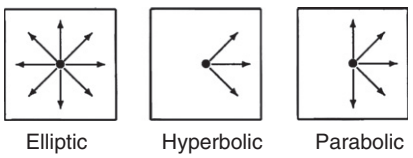

Figure 1.2:
A disturbance propagates differently depending on the type of field equation

1.4.2. Basic CFD Techniques

CFD comprises methods that solve the basic field equations subject to boundary conditions by approaches involving a large number of (mathematically simple) elements. These approaches lead automatically to a large number of unknowns.

Basic CFD techniques are:

- *Boundary element methods (BEM).* BEM are used for potential flows. For potential flows, the integrals over the whole fluid domain can be transformed to integrals over the boundaries of the fluid domain. The step from space (3-d) to surface (2-d) simplifies grid generation and often accelerates computations. Therefore practical applications for potential flows about ships (e.g. wave resistance problems) use exclusively BEM, which are called panel methods. Panel methods divide the surface of a ship (and often part of the surrounding water surface) into discrete elements (panels). Each of these elements automatically fulfills the Laplace equation. Indirect methods determine the element strengths so that at the collocation points (usually centers of the panels) a linear boundary condition (e.g. zero normal velocity) is fulfilled. This involves the solution of a full system of linear equations with the source strengths as unknowns. The required velocities are computed in a second step, hence 'indirect' method. Bernoulli's equation then yields the pressure field. Direct methods determine the potential directly. They are less suited for boundary conditions involving higher derivatives of the potential, but yield higher accuracy for lifting flows. Most commercially used codes for ship flows are based on indirect methods. BEM cannot be used to solve RANSE or Euler equations. Fundamentals of BEM can be found in, e.g., Hess (1986, 1990).
- *Finite element methods (FEM).* FEM dominate structural analysis. For ship hydrodynamics they play only a minor role. Unlike in structural analysis, the elementary functions cannot also be used as weight functions to determine the weighted error integrals (residuals) in a Galerkin method. This reduces the elegance of the method considerably. Fundamentals of FEM can be found in, e.g., Chung (1978).
- *Finite difference methods (FDM).* FDM discretize (like FEM) the whole fluid domain. The derivatives in the field equations are approximated by finite differences. Discretization errors can lead to a violation of conservation of mass or momentum, i.e. in the course of a simulation the amount of water might diminish continuously. While FDM lose popularity and finite volume methods (FVM) gain popularity, in many cases FDM give results of comparable quality.
- *Finite volume methods (FVM).* FVM also employ finite differences for the spatial and temporal discretization. However, they integrate the equations for mass and momentum conservation over the individual cell before variables are approximated by values at the cell centers. This ensures conservativeness, i.e. mass and momentum are conserved because errors at the exit face of a cell cancel with errors at the entry face of the neighbor

cell. Most commercial RANSE solvers today are based on FVM. Fundamentals of FVM can be found in Versteeg and Malalasekera (1995), and Ferziger and Peric (1996).

FEM, FDM, and FVM are called 'field methods', because they all discretize the whole fluid domain (field) as opposed to BEM, which just discretize the boundaries.

Some textbooks on CFD also include spectral methods which use harmonic functions as elementary solutions. Spectral methods have no practical relevance for ship flows. The interested reader will find an introduction in Peyret and Taylor (1985).

1.4.3. Applications

Practical CFD applications for ship flows concentrate mainly on the ship moving steadily ahead. A 1994 survey at ship model basins showed inviscid BEM computations for wave-resistance and offshore seakeeping as still the most important CFD application for commercial projects (ca. 40−50% of the turnover), followed by RANSE applications (30−40%) and computations for propellers (10−20%). All other applications combined contribute less than 5% of the turnover in the commercial sector. This global decomposition has remained remarkably stable despite an overall increase in CFD volume. Besides global aspects like resistance, sometimes local flow details are the focus of attention, e.g. the design of shaft brackets, stabilizing fins, or sonar domes (noise reduction), e.g. Larsson et al. (1998) and Larsson (1997).

The most important applications are briefly discussed in the following.

- *'Resistance and propulsion'*. CFD applications are mainly concerned with steadily advancing ships. For a double-body potential flow, where the wave-making at the free surface and the effects of viscosity are neglected, the flow computation is relatively simple, quick, and accurate. The name 'double-body flow' comes from an interpretation that the ship's hull is reflected at the waterline at rest. Then the flow in an infinite fluid domain is computed and the lower half of the flow gives automatically the flow about a ship with an undeformed (rigid) water surface. The double-body potential flow is only used as an approximate solution for other methods (boundary layer, wave resistance, seakeeping). The simultaneous consideration of viscosity and wave-making drifted into industry applications after the year 2000. But even a decade later, many viscous flow computations in practice still neglected wave-making. For steady free-surface flows ('wave-resistance problem'), inviscid BEM codes are still the workhorse. The propeller is almost always neglected in BEM computations for the steady flow ('resistance problem'). RANSE computations include the propeller action ('propulsion problem'), usually by applying an equivalent body force in the r.h.s. of the RANSE. The body forces were traditionally prescribed based on experience or experimental results. More sophisticated applications used integrated propeller models. The body forces in both thrust and rotative directions are

then estimated, e.g. by a panel method. The distributions obtained by this approach depend on the propeller inflow and are determined iteratively using the RANSE data as input for the propeller computation and vice versa. The approach usually converges quickly.

- *Maneuvering.* Aspects of maneuvering properties of ships gain in importance, as public opinion and legislation are more sensitive concerning safety issues after spectacular accidents of tankers and ferries. IMO regulations concerning the (documented) maneuverability of ships increased the demand for CFD methods in this field. Model tests as an alternative method are expensive and time-consuming. Traditional simple simulation methods with hydrodynamic coefficients gained from analytical approaches or regression analysis (of usually small databases) are often considered as too inaccurate. CFD applications to simulate maneuvering model tests have progressed considerably over the last decade. However, it is difficult to assess the state of the art. By 2010, several research groups presented full maneuvers simulated in RANSE computations. Some companies used by 2010 CFD rather than model tests to furnish maneuvering models to nautical simulators. Yet at the same time, validation workshops showed disappointingly large scatter of results between different simulations. CFD for ship maneuvering appears to be a threshold technology, where we may need another decade before wider confidence in CFD as preferred technique will be established in the industry. Predicting the flow around the hull and appendages (including propellers and rudders) is much more complicated than predicting the steady flow in resistance and propulsion problems. Often, both viscosity and free-surface effects (e.g. dynamic trim and sinkage) play an important role. The rudder is most likely in the hull boundary layer, often operating in the propeller wake. The hull forces themselves are also difficult to predict computationally, because sway and yaw motions induce considerable cross-flows with shedding of strong vortices. Both BEM and field methods have been employed for selected maneuvering problems. Selected problems like side forces and moments in steady yaw are well predicted, but longitudinal forces and some flow details still showed considerable errors for real ship geometries.
- *Ship seakeeping.* The 1990s saw the advent of Rankine panel methods for seakeeping. The approaches are similar to those used for the steady wave-resistance problem, but failed to reach a similar level of acceptance. Most properties of practical relevance are calculated accurately enough for most ship types by strip methods, although the underlying physical models are generally considered as crude. The two-dimensional flow calculations for the individual strips today are based almost always on BEM, namely close-fit methods. RANSE methods for global ship motions have matured over the past decade to industry application. These simulations are applied when strong non-linearities are involved, e.g. green water on deck.
- *Slamming/water-entry problems.* Using suitable space−time transformations, the water entry of a two-dimensional wedge can also be used to model the hydrodynamics of

planing hulls. We will focus here on the seakeeping aspect of modeling water-entry problems. Slamming involves local loads changing rapidly in time and space. Hydroelastic effects, interaction between trapped air pockets and water, velocities that require consideration of water compressibility with shockwaves forming and the complex shapes of the water surface forming jets, make slamming problems already in two dimensions very challenging. Traditional approaches work well for wedges of suitable deadrise angle and two-dimensional flows. But usually ship cross-sections do not have suitable deadrise angles and the phenomena are three-dimensional. CFD has brought substantial progress in this field. Free-surface RANSE simulations are today standard industry practice to predict slamming loads. The focus lies here on forces and deformations, not local pressures. Similarly, sloshing analyses (= internal impact problem) are based on free-surface RANSE simulations.

- *Zero-speed seakeeping.* For offshore applications, global loads and motions in seakeeping can be computed quite well by BEM. For zero speed, the steady wave system vanishes and various diffraction and radiation wave systems coincide. If the geometries of offshore structure and waves are of the same order of magnitude BEM can successfully capture three-dimensional effects and complex interactions. The employed three-dimensional BEM determine forces and motions either in the time or the frequency domain. First-order forces and motions are calculated reliably and accurately. For practically required accuracy of first-order quantities, 1000−2000 elements are typically deemed sufficient. Commercial program packages (WAMIT, TIMIT, AQWA, or DIODORE) are widely accepted and used for offshore applications.
- *Propeller flows.* Inviscid flow methods have long been used in propeller design as a standard tool yielding information comparable to experiments. Lifting-surface methods and BEMs are equally popular. Lifting-surface methods (quasi-continuous method, vortex-lattice method) allow the three-dimensional modeling of the propeller. They discretize the mean camber surface of the propeller blade by individual vortex panels. In addition, the free vortices are modeled by elements of given strength. Other than the BEM described below, lifting-surface methods do not fulfill exactly the boundary conditions at the blade's lower and upper surfaces. However, the resulting errors are small for thin blades. BEM represent an improvement concerning the treatment and modeling of the geometry. BEM model both lift and displacement of the propeller blades by surface panels and/or dipoles. They can also model the propeller hub. Despite the theoretical superiority, BEM results were not clearly better than lifting-surface method results in benchmark tests. BEM codes for propeller applications often use only dipole panels which are distributed over hub, blade surfaces, and the wakes of each blade. Viscous flow CFD methods are applied by industry for complex configurations. Considerable progress in propulsive efficiency is expected when propellers are designed modeling ship, propeller and rudder together, for full scale, with CFD. This is expected to become industry standard practice by 2030.

Further, less frequently found applications of CFD in naval architecture include:

- *Air flow.* CFD has been applied to air flows around the upper hull and superstructure of ships and offshore platforms. Topics of interest are:
  - Wind resistance (especially of fast ships)
    For fast ships the wind resistance becomes important. For example, for one project of a 50 knot SES (surface effect ship = air-cushion catamaran), the wind resistance constituted ca. 25% of the total resistance. Hull changes limited to the bow decreased the wind resistance by 40%.
  - Wind-over-the-deck conditions for helicopter landing
    This application concerns both combatants and offshore platforms.
  - Wind loads
    Wind loads are important for ships with large superstructures and relatively small lateral underwater area, e.g. car transporters, car ferries, container ships, SES, and air-cushion vehicles.
  - Tracing of funnel smoke
    This is important for passenger vessels (passengers on deck, paintwork) and for offshore platforms (safety of helicopter operation). Formal optimization has been combined with CFD to minimize smoke dispersion on the deck of a yacht (Harries and Vesting 2010).

  The comparison of CFD, wind-tunnel tests, and full-scale measurements shows an overall good agreement, even if large discrepancies appear at some wind directions. The differences between CFD and model-test results are not generally larger than between full-scale and model-scale results. In fact, the differences are not much larger than often found when the same vessel is tested in different wind tunnels. The determination of wind loads on ships and offshore structures by CFD is a realistic alternative to the experimental methods.
- *Interior flows.* Sloshing in partially filled tanks is a standard CFD application, and required by classification societies for some cases. Sloshing computations may be coupled to the outer (global) motions of a ship, but industry practice uses only weak coupling: the global ship motions are prescribed for the tank, but the effect of the fluid motion in the tank on the global ship motions is neglected. Related problems are flows in a roll damping tank and water flowing into a damaged ship.

Table 1.1 summarizes an assessment of the maturity of the various CFD applications.

1.4.4. Cost and Value Aspects of CFD

The value of any product (or service) can be classified according to time, cost, and quality aspects. For CFD this means:

- *Time benefits* (How does CFD accelerate processes in ship design?). In the shipbuilding industry, we see the same trends towards ever-decreasing times for product development

Table 1.1: Maturity of CFD application on a scale from – (not applicable, no applications known) to •••• (very mature)

	Viscous	Inviscid
'Resistance test'	•••	•••
'Propulsion test'	•••	–
Maneuvering	•	•
Ship seakeeping	••	•••
Offshore	•	•••
Propeller	••	••••
Others	••	–

as in other manufacturing industries. In some cases, delivery time is the key factor for getting the contract. CFD plays a special role in this context. A numerical pre-optimization can save time-consuming iterations in model tests and may thus reduce total development time. The speed of CFD allows applications already in preliminary design. Early use thus reduces development risks for new ships. This is especially important when exploring niche markets for unconventional ships where design cannot be based on experience. In addition, another aspect related to turnover has to be realized: CFD improves chances of successful negotiations by supplying hydrodynamic analyses. It has become standard for all high-tech shipbuilders to apply at least inviscid CFD analyses to proposed hull designs when entering negotiations to obtain a contract for building a ship.

- *Quality benefits* (How does CFD enable superior ships or reduce risks in new designs?). Model tests are still more accurate for power prognosis than CFD. We see occasionally good agreement of CFD power prediction with measured data, but these cases may just benefit from fortunate error cancellation or tuning of parameters to fit a posteriori the experimental data. No 'blind' benchmark test has yet demonstrated the ability of CFD codes to predict, at least with 5% accuracy, consistently the power of ship hulls at design speed. I expect this to remain so for some more years. In the long run, CFD should outperform model tests, as with growing computational power, accurate simulations at full scale will become available overcoming current uncertainties in correlating model tests to full-scale predictions. For some projects, it is only important to ensure that a given installed power will enable the ship to achieve contract speed. In these cases, CFD is of little interest. However, CFD should be considered in cases where model test results show problems or the shipowner is willing to pay a higher price for lower operating costs (due to improved hull). CFD allows insight in flow details not offered by the standard model tests. Insight in flow details is especially important in cases where initial model tests show that power requirements for a given hull are far more than expected. Here CFD also allows the investigation of the flow far below the waterline and modifications can be quickly analyzed to see if major improvements are to be expected. The model tests and experience of a towing tank mainly indicate the potential for improvement; CFD indicates where and

how to improve the design. CFD also allows formal optimization, using hundreds of 'numerical towing tanks' in parallel.

- *Cost benefits* (How does CFD reduce costs in ship designs?). While the influence of certain decisions and actions on the turnover can be estimated only qualitatively, costs can usually be quantified directly. This explains why management prefers investments with a short payback due to cost reductions even though there is general consent that cost reductions alone do not ensure the economic future of a company. However, CFD's potential for direct cost reductions is small. CFD is still considered widely as not accurate enough to substitute the model test for power prognosis. Therefore, *one* model test is always performed. In three out of four projects of the Hamburg Ship Model Basin this was sufficient already in 1990. By 2010, a single model test trial had become standard practice. Thus, there is little direct cost reduction potential. Indirect cost savings in other departments are difficult to quantify. Time benefits of CFD will also affect costs. It is possible to determine 40−60% of the total production costs of a ship in the first weeks of design. Costs for modifications in later stages are higher by order of magnitudes than those necessary at the conceptual phase. Various decisions concerning production costs can be made earlier and involve lower risks if CFD is employed consistently to determine the final hull form at an earlier time.

The benefits discussed so far only cover one-half of a cost−benefit analysis for a CFD strategy. Understanding the cost structure of CFD is at least as important and some general management guidelines can be deduced. This requires a closer look at the work process in CFD. The work process is split into:

- preprocessing (generation and quality control of grids);
- computation;
- postprocessing (graphical displays, documentation).

The individual steps sometimes have to be performed several times in iterations. Cost structures will be discussed separately for each step:

1. *Preprocessing.* Preprocessing requires staff familiar with the special programs for grid generation, especially on the hull. This requires at least a basic understanding of the subsequent CFD computation. Grid generation is best performed on workstations or fast PCs with high-resolution screens. User experience and a degree of automation mainly determine time (and labor) costs in this step. Progress in grid generation and more robust CFD has reduced the man time involved in CFD analyses. Largely automatic procedures are now available for many applications. Staff training and grid generation software are the main fixed costs in this step.
2. *Computation.* The computation involves almost no man time. Computations for inviscid CFD can usually run on PCs; viscous CFD and formal optimization require more powerful computer environments with parallel computing. Computing costs usually

account for less than 1% of total costs. Also, software licenses for the flow code are often negligible compared to other costs, especially those for training (Bertram and Couser 2010).

3. *Postprocessing.* Postprocessing is generally based on commercial software. Postprocessing requires some time (typically 10−30% of the total time). Increasingly, videos are used for unsteady CFD applications. Interpretation of results still requires expertise. You pay thus for the skilled interpretation, not the number of color plots.

The high fixed costs for training and user-defined macros to accelerate the CFD process lead to considerable economies of scale. This is often not realized by management. Experience shows that many shipyards buy CFD software, because the hardware is available or not expensive, and the software license costs may be as much as a few CFD analyses at a consulting company. The vendors are naturally only too happy to sell the software. Then the problems and the disillusion start. Usually no initial training is given by the vendor (or bought by the shipyard). Typical beginners' mistakes are the consequence:

- Time is lost in program handling
- Unsuitable models and grids are used requiring repeated analyses or leading to useless results.

By the time the management realizes the problems, it is usually too late. The software licenses are all bought, the design engineer has now already invested (lost) so much time struggling with the code. Nobody wants to admit defeat. So the CFD analyses are continued in-house with the occasional outsourcing when problems and time pressures become too large. As a general rule, outsourcing is recommended for shipyards and design offices with fewer than five projects per year. In-house CFD makes sense starting from ten projects per year. For finite-element analyses of structures we have seen a development that after an initial period where shipyards performed the analyses in-house the pendulum swung the other way with shipyards now using almost exclusively outsourcing as the sensible option. A similar development is expected for most specialized CFD applications.

Model generation plays a vital role for costs, response time, and quality of results. In this respect, CFD analyses have benefited considerably from the progress in guided or automated grid generation since the year 2000.

- *By making grid generation more user-friendly.* Grid generation was largely a matter of experience. The logical deduction was to incorporate this experience in the grid generation codes to improve user-friendliness. A fundamental dilemma found in model generation is that the procedures should be flexible to cope with a variety of problems, yet easy to handle with a minimum of input. Many flow codes offer a lot of flexibility, often at the cost of having many options which in turn leave inexperienced (i.e. occasional) users frustrated and at risk to choose exactly the wrong options for their problems. Incorporation

of expert knowledge in the model generation program offering reasonable default options is a good solution to this dilemma. In the extreme case, a user may choose the 'automatic mode' where the program proceeds completely on its own knowledge. On the other hand, default values may be overruled at any stage by an experienced user.

- *By making the computation more robust.* A simple grid is cheap and fast to generate, but unsuitable for most marine problems. Therefore modern, marine CFD applications use:
  - block-structured grids, sometimes with sliding block interfaces;
  - non-matching boundaries between blocks;
  - unstructured grids;
  - chimera grids (overlapping, non-matching blocks).
- *By generating grids only once.* Time for grid generation means *total* time for all grids generated. The philosophy is to 'Get it right the first time', i.e. the codes are robust enough or the grid generators good enough that grids need to be created only once. This should also favor the eventual development of commercial codes with adaptive grid techniques. First industrial applications to ships appeared around 2010.

Standard postprocessing could save time and would also help customers in comparing results for various ships. However, at present we have at best internal company standards on how to display CFD results.

1.5. Viscous Flow Computations

Fundamentals of viscous flows are covered in detail in Ferziger and Peric (1996). Fundamentals of potential flow methods are found on the website. I will therefore limit myself here to a naval architect's view of the most important issues for applications of these methods. This is intended to raise the understanding of the matter to a level sufficient to communicate and collaborate with a CFD expert.

1.5.1. Turbulence Models

The RANSE equations require external turbulence models to couple the Reynolds stresses (terms from the turbulent fluctuations) to the time-averaged velocities. Turbulence is in general not fully understood. All turbulence models used for ship flows are semi-empirical. They use some theories about the physics of turbulence and supply the missing information by empirical constants. None of the turbulence models used so far for ship flows has been investigated for its suitability at the free surface. On the other hand, it is not clear whether an exact turbulence modeling in the whole fluid domain is necessary for engineering purposes. There are whole books on turbulence models and we will discuss here only the most popular turbulence models, which are standard options in commercial RANSE solvers. ITTC (1990) gives a literature review of turbulence models as applied to ship flows.

Turbulence models may be either algebraic (0-equation models) or based on one or more differential equations (one-equation models, two-equation models, etc.). Algebraic models compute the Reynolds stresses directly by an algebraic expression. The other models require the parallel solution of additional differential equations which is more time consuming, but also more accurate.

The six Reynolds stresses (or more precisely their derivatives) introduce six further unknowns. Traditionally, the Boussinesq approach has been used in practice which assumes isotropic turbulence, i.e. the turbulence properties are independent of the spatial direction. (Detailed measurements of ship models have shown that this is not true in some critical areas in the aftbody of full ships. It is unclear how the assumption of isotropic turbulence affects global properties like the wake in the propeller plane.) The Boussinesq approach then couples the Reynolds stresses to the gradient of the average velocities by an eddy viscosity μ_t:

$$-\rho\begin{bmatrix}\overline{u'u'} & \overline{v'u'} & \overline{w'u'}\\ \overline{u'v'} & \overline{v'v'} & \overline{w'v'}\\ \overline{u'w'} & \overline{v'w'} & \overline{w'w'}\end{bmatrix} = \mu_t\begin{bmatrix}2u_x & u_y+v_x & u_z+w_x\\ u_y+v_x & 2v_y & w_y+v_z\\ u_z+w_x & w_y+v_z & 2w_z\end{bmatrix} - \begin{bmatrix}\frac{2}{3}\rho k & 0 & 0\\ 0 & \frac{2}{3}\rho k & 0\\ 0 & 0 & \frac{2}{3}\rho k\end{bmatrix} \tag{1.38}$$

where k is the (average) kinetic energy of the turbulence:

$$k = \frac{1}{2}(\overline{u}^2 + \overline{v}^2 + \overline{w}^2) \tag{1.39}$$

The eddy viscosity μ_t has the same dimension as the real viscosity μ, but unlike μ it is not a constant, but a scalar depending on the velocity field. The eddy viscosity approach transforms the RANSE to:

$$\begin{aligned}
\rho(u_t + uu_x + vu_y + wu_z) &= \rho f_1 - p_x - \frac{2}{3}\rho k_x + (\mu+\mu_t)(u_{xx}+u_{yy}+u_{zz})\\
&\quad +\mu_{tx}2u_x + \mu_{ty}(u_y+v_x) + \mu_{tz}(u_z+w_x)\\
\rho(v_t + uv_x + vv_y + wv_z) &= \rho f_2 - p_y - \frac{2}{3}\rho k_y + (\mu+\mu_t)(v_{xx}+v_{yy}+v_{zz})\\
&\quad + \mu_{tx}(u_y+v_x) + \mu_{ty}2v_y + \mu_{tz}(w_y+v_z)\\
\rho(w_t + uw_x + vw_y + ww_z) &= \rho f_3 - p_z - \frac{2}{3}\rho k_z + (\mu+\mu_t)(w_{xx}+w_{yy}+w_{zz})\\
&\quad + \mu_{tx}(u_z+w_x) + \mu_{ty}(w_y+v_z) + \mu_{tz}2w_z
\end{aligned} \tag{1.40}$$

Turbulence models generally use a reference length scale and reference velocity scale. Alternatively, the velocity scale can be expressed as the fraction of length scale and a time

scale. To obtain the proper dimension, the eddy viscosity is expressed proportional to the product of length scale and velocity scale. The length scale is characteristic for the larger turbulence structures which are mainly contributing to the momentum transfer in the fluid. The velocity scale is characteristic for the intensity of the turbulent fluctuations.

All commonly used turbulence models are plagued by considerable uncertainties. Internationally renowned fluid dynamicists have described turbulence models as follows:

- 'Turbulence models are voodoo. We still don't know how to model turbulence.'
- 'The word "model" is a euphemism for an uncertain, but useful postulated regularity. In the last few decades, scientists have learned to simulate some aspects of turbulence effects by the invention of "turbulence models" which purport to represent the phenomena by postulated laws of conservation, transport and sources for supposed "properties of turbulence" such as its "energy", its "frequency" or its "length scale". These "laws" are highly speculative.'

Researchers have succeeded in direct numerical simulation of turbulence for Reynolds numbers several orders of magnitude smaller than ship model Reynolds numbers and for very simple geometries. These simulations allow one at best to understand phenomena of turbulence better and to test engineering turbulence models.

The usefulness of a turbulence model for ship flows can only be evaluated in benchmark tests for similar ships. Sometimes simple models work surprisingly well; sometimes the same model fails for the next ship. The most popular turbulence model for ship flow applications in practice remains the standard $k-\varepsilon$ model, although its results were not convincing in benchmark tests for several ship geometries.

By the late 1990s, $k-\omega$ models were proposed for ship flows. These models are like the $k-\varepsilon$ two-equation models and can be seen as a further evolution of them. ω is proportional to ε/k and can be interpreted as a 'turbulence frequency'. $k-\omega$ models yield better agreement with experiments in many cases; however, they react more sensitively to grid quality.

Reynolds stress models calculate the individual Reynolds stresses from their modeled transport equations without recourse to an eddy viscosity hypothesis. These models require more computational effort than, e.g., the two-equation $k-\varepsilon$ model, but showed superior results in several ship flow applications. However, it is not yet decided if similarly good results can be obtained by simple turbulence models with properly adjusted coefficients.

Large-eddy simulations may eventually solve the current debate over turbulence modeling for engineering applications, but for ship flows we will have to wait at least two more decades before realistic LES solutions become available in practice.

Probably the most widely used turbulence model in engineering applications is the (standard) $k-\varepsilon$ model (Launder and Spalding 1974). k is the kinetic energy of the turbulence, ε the dissipation rate of k. The $k-\varepsilon$ model expresses the eddy viscosity μ_t as a simple function of k and ε:

$$\mu_x = 0.09\rho \frac{k^2}{\varepsilon} \tag{1.41}$$

where 0.09 is an empirical constant. k and ε are expressed by two partial differential equations involving further empirical constants:

$$\frac{\mathrm{D}k}{\mathrm{D}t} = \frac{1}{\rho}\left(\left(\frac{\mu_t}{1.0}k_x\right)_x + \left(\frac{\mu_t}{1.0}k_y\right)_y + \left(\frac{\mu_t}{1.0}k_z\right)_z \right) + P_k - \varepsilon \tag{1.42}$$

$$\frac{\mathrm{D}\varepsilon}{\mathrm{D}t} = \frac{1}{\rho}\left(\left(\frac{\mu_t}{1.2}\varepsilon_x\right)_x + \left(\frac{\mu_t}{1.2}\varepsilon_y\right)_y + \left(\frac{\mu_t}{1.2}\varepsilon_z\right)_z \right) + 1.44\frac{\varepsilon}{k}P_k - 1.92\frac{\varepsilon^2}{k} \tag{1.43}$$

P_k is the production rate of k:

$$\begin{aligned} P_k = \frac{\mu_t}{\rho}\,(&2u_x u_x + (u_y + v_x)u_y + (u_z + w_x)u_z + (v_x + u_y)v_x + 2v_y v_y \\ &+ (v_z + w_y)v_z + (w_x + u_z)w_x + (w_y + v_z)w_y + 2w_z w_z) \end{aligned} \tag{1.44}$$

The substantial derivative is defined as usual:

$$\frac{\mathrm{D}}{\mathrm{D}t} = \frac{\partial}{\partial t} + u\frac{\partial}{\partial x} + v\frac{\partial}{\partial y} + w\frac{\partial}{\partial z} \tag{1.45}$$

These equations contain four empirical constants (1.0, 1.2, 1.44, and 1.92) which were determined (in a best fit approach) for very simple flows in physical and numerical experiments. The applicability to other turbulent flows (e.g. around ship geometries) was never explicitly validated.

The $k-\varepsilon$ model cannot be applied directly at a wall (ship hull) as it assumes inherently high (local) Reynolds numbers. If a no-slip condition (zero relative speed at the hull) is to be enforced directly at the wall, the ε differential equation must be substituted by an algebraic equation near the wall. This is the so-called low-Re $k-\varepsilon$ model. However, more popular is the introduction of a wall function coupled to the standard $k-\varepsilon$ model. The wall function is empirically determined for two-dimensional flows. One assumes that the velocity increases logarithmically with distance from the wall:

$$\frac{u}{u_\tau} = \begin{cases} y^+ & y^+ \le y_m^+ \\ \dfrac{1}{0.42}\ln(9.0y^+) & y^+ > y_m^+ \end{cases} \tag{1.46}$$

where y_m + is implicitly given by:

$$y_m^+ = \frac{1}{0.42} \ln(9.0 y_m^+) \tag{1.47}$$

0.42 and 9.0 are empirical constants. $y^+ = y\rho u_\tau/\mu$ is a non-dimensional distance from the wall, u the velocity in longitudinal (parallel to the wall) direction, $u_\tau = \sqrt{\tau_w/\rho}$ with τ_w the wall shear stress.

The centers of the innermost cells should lie within a distance from the wall where the logarithmic law of the wall function applies, i.e. $100 < y^+ < 1000$. However, y^+ contains the wall shear stress, which is part of the solution and not a priori known. It is thus only possible to judge a posteriori if a chosen wall distance was appropriate. Higher Reynolds numbers require generally smaller y^+.

The fundamental assumptions for the wall function are:

- velocity gradient in normal direction is much larger than in other directions;
- pressure gradient and gravity influence are so small that shear stresses in the boundary layer are constant;
- shear stresses and velocity vectors have the same direction in the whole boundary layer;
- equilibrium of turbulence generation and dissipation;
- linear variation of the reference length for turbulence.

These assumptions are questionable for complex flows as found in the aftbodies of ships. The standard $k-\varepsilon$ model usually over-predicts the turbulent kinetic energy in the stern region. Also, the model cannot properly account for the reduction of the turbulent kinetic energy near the wall when the viscous layer becomes thick over the stern. The wall function approach usually yields worse results for the wall shear stresses than turbulence models that apply a no-slip condition directly at the wall. However, the wall function saves many cells (and thus computational time).

The $k-\varepsilon$ model appears suitable for flows with a predominant boundary-layer character. Problems with defining a reference length, as in many algebraic models, are avoided and at least the important physical aspect of turbulence transport is explicitly reflected in the model. The wall function makes the approach numerically efficient, but the model is in principle not capable of predicting flow separation for curved surfaces (e.g. ships!).

1.5.2. Boundary Conditions

The computational grid can only cover part of the real fluid domain. This introduces artificial boundaries of the computational domain in addition to the physical boundaries of the hull and the free surface.

For ships moving straight ahead (as in simulations of resistance or propulsion tests), the midship plane is generally treated as a symmetry plane. The usual symmetry of the ship would intuitively suggest that this indeed reflects physical reality. However, viscous flows with symmetric inflow to symmetric bodies do not automatically result in symmetric flow patterns at all times. Vortex shedding results in asymmetric flow patterns which only in the time average are symmetric again. This may result in considerable differences in the resistance. The following example may illustrate the problem (Fig. 1.3). Behind a circular cylinder in uniform inflow one would assume intuitively a symmetrical flow which would hardly be disturbed by a flat plate behind the cylinder. However, experiments yield a considerably smaller resistance coefficient for the cylinder with a flat plate. The reason is vortex shedding behind the cylinder with large vortices oscillating from one side to the other. These large-vortex oscillations are blocked by the flat plate.

The boundary condition on the hull is a no-slip condition (zero relative speed) which is either enforced directly or via a wall function depending on the turbulence model employed.

The side and bottom boundaries may correspond to an actual physical boundary as in a model tank. In this case, the boundaries may be treated similar to the ship hull with a no-slip condition. However, one should remember that the outer boundaries then have a relative velocity to the ship. Usually, the physical boundaries would be too far away to be considered. Then the side and bottom boundaries should be sufficiently removed from the ship. Often the side and bottom boundaries form part of a cylinder (quarter for double-body flow with symmetry in y), as a cylinder usually leads to better grids (for single-block grids) than a block-type grid. A typical cylinder radius is one ship length.

At the inlet all unknowns are specified. If the inlet is chosen sufficiently upstream of the ship, uniform flow with corresponding hydrostatic pressure can be assumed. If the $k-\varepsilon$ model is employed, the distributions of k and ε at the inlet also have to be specified. The influence of the specified values for k and ε decays rapidly downstream, such that errors have decayed by some

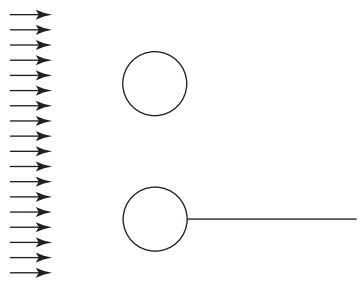

Figure 1.3:
A cylinder with a flat plate in the wake has a considerably lower resistance coefficient than a cylinder without a plate. Care is required when assuming symmetry planes for viscous flow computations

orders of magnitude after several cells. One may then simply specify zero k and ε. A slightly more sophisticated approach estimates the turbulence intensity I (turbulent fluctuation component of a velocity component made non-dimensional with the ship speed V) at the inlet. For isotropic turbulence we then get:

$$k = \frac{3}{2}(VI)^2 \tag{1.48}$$

In the absence of experimental data for I in a specific case, $I = 5\%$ has often been assumed. The dissipation rate is typically assumed as:

$$\varepsilon = 0.164 \frac{k^{1.5}}{\ell} \tag{1.49}$$

where 0.164 is an empirical constant and ℓ a reference length. For ship flows, there are few indications as to how to choose this reference length. Our own computations have used 1/100th of the radius of the cylinder forming the computational domain. However, the initial choice of the quantities does not influence the final result, but 'only' the required number of iterations to obtain this result. If only the aftbody is considered, then the inlet may be placed, for example, amidships. In this case all unknowns must be specified from experiments (for validation studies) or simpler computations (e.g. coarse grid computations for the whole domain, inviscid flow computations coupled with boundary layer computations, etc.).

At the outlet usually the derivatives in the longitudinal direction are set for all unknowns to zero and the flow leaving the domain is determined such that continuity is preserved for the whole fluid domain. The longitudinal derivatives are in reality not zero, but this boundary condition prevents upstream propagation of any reflections of disturbances created by the numerical method. Numerical experiments show that these boundary conditions affect results only in a small local region near the outlet.

At symmetry planes normal velocity and all derivatives in the normal direction are set to zero. Since the normal derivatives of the tangential velocities vanish, the shear stresses are zero. The outer boundary of the computational domain (side and bottom) may be treated as 'symmetry plane', i.e. on each outer cell face normal velocity and all normal derivatives are set zero. In this case, the outer boundary must be far away from the ship such that virtually uniform flow is encountered. Another possibility is to specify values computed by inviscid codes at the outer boundary, which allows much smaller computational domains, but not many fewer cells as most cells are concentrated near the ship hull.

If a propeller is modeled in RANSE computations for ship flows (propulsion test condition), it is generally simplified by specifying the propeller effect as body forces. This simulates the acceleration of the flow by the propeller. The sum of all axial body forces yields the thrust. The distribution is often assumed to be parabolic in the radial direction and constant in the

circumferential direction. Alternatively, the distribution of the body forces for the propeller may be specified from:

- experience with similar ships;
- experiments for the actual ship;
- alternating computations for the propeller loading with non-uniform inflow from the RANSE computation. The propeller loading is then computed every 10 or 20 iterations in the RANSE computation as the propeller loading converges much faster than the other properties of the RANSE computation. Convergence for the propeller loading is usually obtained with five or seven iterations.

1.5.3. Free-Surface Treatment

Most viscous flow computations for ships in design projects in the 1990s still assumed the free surface to be a symmetry plane. In reality this is not true. The free surface forms waves which break locally at the bow, and the ship changes trim and sinkage (squat) due to the free surface. The problem of turbulence models (and their specific boundary conditions) near the free surface has not been addressed in ship flows and generally the same conditions as for symmetry planes are used.

A variety of methods exists to capture wave-making with various degrees of success. The difficulty with the unknown free-surface position is usually resolved by considering the problem transient, starting from rest. The hull is thus accelerated to the requested Froude number and the time integration is continued until steady state conditions have been achieved. (This procedure corresponds to usual practice in towing tank experiments.) The free-surface position is updated as part of the iterative process.

The methods for computing flows with a free surface can be classified into two major groups:

- Interface-tracking methods define the free surface as a sharp interface whose motion is followed. They use moving grids fitted to the free surface and compute the flow of liquid only. Problems are encountered when the free surface starts folding or when the grid has to be moved along walls of a complicated shape (like a real ship hull geometry).
- Interface-capturing methods do not define a sharp boundary between liquid and gas and use grids which cover both liquid- and gas-filled regions. Either marker particles or a transport equation for the void fraction of the liquid phase are used to capture the free surface.

Interface tracking has become the standard approach as the ability to model complex geometries of hull and water surface is essential for real ship flows. Interface-tracking methods may also solve the flow in the air above the water, but for most ship flows this is not necessary.

A typical approach uses an extended volume-of-fluid (VOF) formulation introducing an additional scalar function, which describes the volume concentration of water, to identify the position of the free surface.

Initial problems with numerical damping of the ship wave propagation have been overcome by better spatial resolution and using higher-order schemes.

1.5.4. Further Details

The vector equations for conservation of momentum yield three scalar equations for three-dimensional computations. These determine the three velocity components for a given pressure. Usually these velocities do not fulfill the continuity equation. The introduction of a pressure correction equation derived from the continuity equation allows a correction of pressure and velocities. Popular methods for such pressure–velocity coupling are:

- SIMPLE (*s*emi-*im*plicit *p*ressure *l*inked *e*quations) and related methods;
- PISO (*p*ressure *i*mplicit with *s*plitting of *o*perators).

In the 1990s most RANSE codes used for ship flows employed SIMPLE or related pressure–velocity coupling. The SIMPLE method is fast, but tends to slow convergence for suboptimal grids. Figure 1.4 gives a simple flow chart for the SIMPLE algorithm. PISO, like SIMPLE, is based on a predictor–corrector method, but employs several corrector steps while SIMPLE uses only one. This makes the PISO method more stable, but less efficient. In personal experience, the computation time for one tanker was increased by a factor of 5 switching from SIMPLE to PISO. For unsteady problems, however, the PISO method is generally preferred to the SIMPLE method due to its better stability. The discretization of the fundamental differential equations leads to very large systems of linear equations which are usually sparse, i.e. most of the elements of the matrix are zero. (This is fundamentally different from boundary element methods where full matrices with an often not dominant main diagonal need to solved.) Direct solvers like Gauss elimination or matrix inversion have prohibitively excessive computational time and storage requirements. In addition, the solution of the system of equations is embedded in an outer iteration which requires only an approximate solution, because the coefficients due to the non-linearity of the differential equations and the pressure–velocity coupling require further corrections. Therefore field methods generally employ iterative solvers:

- Gauss–Seidel method (point iterative);
- LSOR (line successive overrelaxation), ADI (alternating direction implicit) (line iterative);
- ILU (incomplete lower upper) decomposition, e.g. SIP (strong implicit procedure);
- CG (conjugate gradient) method.

The various iterative methods differ in their prerequisites (dominant main diagonal, symmetry, etc.), convergence properties, and numerical effort per iteration. Strongly implicit schemes

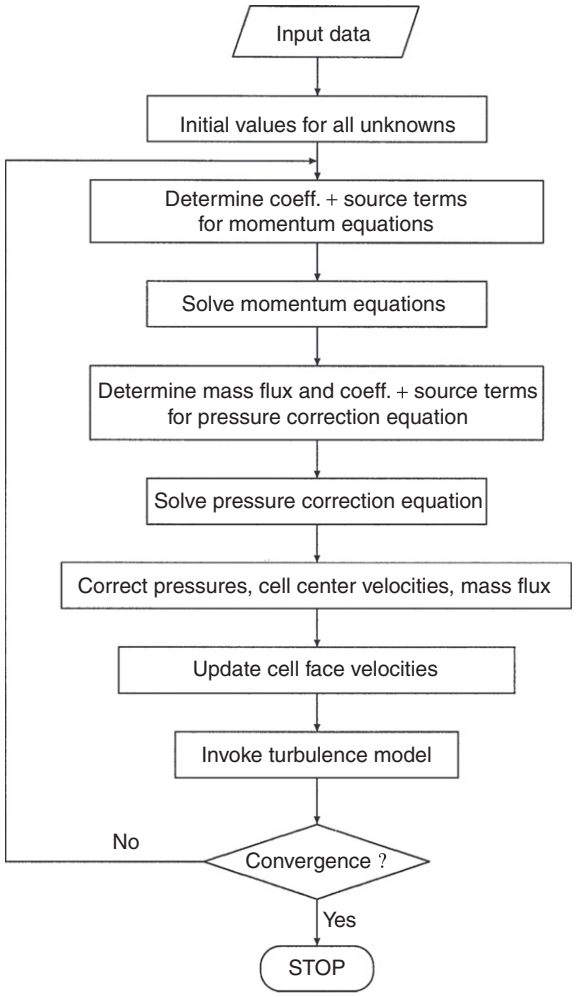

Figure 1.4:
Flow chart for SIMPLE algorithm

such as SIP feature high convergence rates. The convergence is especially high for multigrid acceleration which today is almost a standard choice.

1.5.5. Multigrid Methods

Multigrid methods use several grids of different grid size covering the same computational fluid domain. Iterative solvers determine in each iteration (relaxation) a better approximation to the exact solution. The difference between the exact solution and the approximation is called residual (error). If the residuals are plotted versus the line number of the system of equations, a more or less wavy curve appears for each iterative step. A Fourier analysis of this curve then

yields high-frequency and low-frequency components. High-frequency components of the residual are quickly reduced in all solvers, but the low-frequency components are reduced only slowly. As the frequency is defined relative to the number of unknowns, respectively the grid fineness, a given residual function is highly frequent on a coarse grid, and low frequency on a fine grid. Multigrid methods use this to accelerate overall convergence by the following general procedure:

1. Iteration (relaxation) of the initial system of equations until the residual is a smooth function, i.e. only low-frequent components are left.
2. 'Restriction': transforming the residuals to a coarser grid (e.g. double the grid space).
3. Solution of the residual equation on the coarse grid. Since this grid contains for three-dimensional flow and grid space halving only one-eighth of the unknowns and the residual is relatively high frequency now, only a fraction of the computational time is needed because a further iteration on the original grid would have been necessary for the same accuracy.
4. 'Prolongation': interpolation of the residuals from the coarse grid to the fine grid.
5. Addition of the interpolated residual function to the fine-grid solution.

This procedure describes a simple two-grid method and is recursively repeated to form a multigrid method. If the multigrid method restricts (stepwise) from the finest grid to the coarsest grid and afterwards back to the finest grid, a V-cycle is formed. If the prolongation is only performed to an intermediate level, again before restriction is used, this forms a W-cycle (Fig. 1.5).

The multigrid method accelerates the overall solutions considerably, especially for grids with many unknowns. Multigrid algorithms obtain computational times which are almost proportional to the number of cells, while single-grid solvers yield computational times proportional approximately to the square of the number of cells. Multigrid methods are relatively easy to combine with all major iterative solvers. The considerable speed-up of computations more than justifies the additional expense of programming and storage requirements.

1.5.6. Numerical Approximations

Finite-volume methods require values (and derivatives) of various variables at the cell faces, when they are originally only known at the cell centers. The flow direction is often considered

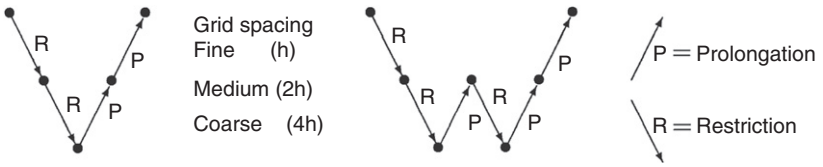

Figure 1.5:
Multigrid cycles: V-cycle (left), W-cycle (right); h: grid spacing computations

when these quantities are determined for convective terms. Time derivatives are also numerically approximated. Consider, for example, the convective fluxes in the x direction. One determines in general the value of a variable (e.g. pressure or velocity) at the location x by employing an interpolation polynomial through the neighboring cell centers x_i:

$$f(x) = a_1 + a_2(x - x_1) + a_3(x - x_1)(x - x_2) + \ldots \tag{1.50}$$

The coefficients a_i are determined by inserting the known function values $f_i = f(x_i)$. The simplest case uses just the value of the next cell centerupstream (*upwind differencing scheme, UDS*):

$$f(x) = \begin{cases} f_{i-1} & u > 0 \\ f_i & u < 0 \end{cases} \tag{1.51}$$

where u is the flow velocity in the x direction. This is a first-order approximation, i.e. (for fine grids) halving the grid size should halve the error in approximating the derivative. The order of an approximation is derived from a Taylor expansion for equidistant grids. For non-equidistant grids, an additional error appears that depends on the ratio of adjacent cell lengths. This error may dominate for coarse to moderately coarse grids, but vanishes in the theoretical limit of infinitely fine grids. The approximation thus depends on the direction of the velocity in the cell center. UDS is unconditionally stable, but plagued by large numerical diffusion. Numerical diffusion smoothes the derivatives (gradients) and may thus lead to wrong results. The numerical diffusion becomes maximal for an angle of 45° between grid lines and flow direction. Grid refinement reduces the numerical diffusion, but increases, of course, the computational effort.

The *central differencing scheme (CDS)* uses the adjacent upstream and downstream points:

$$f(x) = \frac{f_{i-1} + f_i}{2} \tag{1.52}$$

This is a second-order approximation, i.e. halving the grid size will reduce the error by one-quarter for fine grids. The approximation is independent of the sign of the flow direction. CDS tends to numerical instabilities and is therefore (for usual discretizations and speeds) unsuited for the approximation of the convective fluxes; the diffusive terms are usually approximated by CDS.

The *linear upwind differencing scheme (LUDS)* uses the cell centers of the next two upstream points:

$$f(x) = \begin{cases} \dfrac{f_{i-2} - f_{i-1}}{x_{i-2} - x_{i-1}}(x - x_{i-1}) + f_{i-1} & u > 0 \\ \dfrac{f_i - f_{i+1}}{x_i - x_{i+1}}(x - x_i) + f_i & u < 0 \end{cases} \tag{1.53}$$

This second-order approximation considers again the flow direction. LUDS is more stable than CDS, but can yield unphysical results. This is sometimes referred to as 'numerical dispersion'. Three points allow quadratic interpolation. The *QUICK* (*quadratic upstream interpolation for convective kinematics*) uses two adjacent points upstream and one downstream:

$$f(x) = \begin{cases} \dfrac{f_i + f_{i-1}}{2} - \dfrac{1}{8}(f_{i-2} + f_i - 2f_{i-1}) & u > 0 \\ \dfrac{f_i + f_{i-1}}{2} - \dfrac{1}{8}(f_{i+1} + f_{i-1} - 2f_i) & u < 0 \end{cases} \tag{1.54}$$

This third-order approximation may also produce unphysical results due to overshoots and requires a higher computational effort than the other schemes presented so far.

Blended schemes combine the basic schemes in weighted averages. Optimum weight factors depend on the problem. Blending combines the advantages (stability, accuracy) of the individual schemes, but requires more effort in each iteration. For an optimum weight the reduced number of iterations should more than compensate for this. For ship flows our experience is still insufficient to give general recommendations for blending schemes. Ideally, the weighting factors are chosen depending on the local flow. This usually involves the Peclet number, i.e. a local Reynolds number based on the local velocity and the grid size. Even more sophisticated techniques use a basic scheme (e.g. CDS) unless local instabilities (wiggles) are diagnosed automatically. These instabilities are then smoothed or filtered. These schemes do not require (error-prone) user input as do the simpler blending schemes. Blending may also be time-dependent. Then a more robust blend is used in the beginning to ensure numerical stability, and a more accurate blend is used later to obtain accurate converged results.

For the approximation of time derivatives implicit or explicit schemes may be used. In explicit schemes, the variables (e.g. derivatives of velocities) depend at each point in space only on known values of previous time steps. They can thus be computed directly (explicitly). Implicit schemes couple the unknowns to neighboring values (in time) and require the solution of a system of equations. Explicit schemes cannot usually be employed for ship flows, because they require very small time steps for the necessary very fine spatial discretization. A popular implicit scheme is the Crank–Nicholson scheme.

1.5.7. Grid Generation

Model set-up, especially grid generation, is decisive for time, cost, and quality of results in any CFD project. Grids must capture the changes in the geometries of hull and free surface (if included), but also all changes in the flow, with sufficient accuracy. For reasons of computational accuracy and efficiency (convergence rate), one should try to avoid extreme cell side ratios and skewed angles in individual cells. However, for ship flows, the flow changes drastically in the normal direction to the hull and little in the tangential longitudinal direction.

One would like to have a similar resolution for all changes in the flow direction. This automatically forces us to use cells with extreme side ratios, e.g. 1:1000. Grids should be rather fine in regions of high velocity or pressure gradients. The curvature of the ship hull and the experience with similar ship hull forms give some indications where such regions are to be expected, but often one identifies only after computations regions where the grid should have been finer. Ideally the computation should refine the grid in these regions automatically during a computation. Such adaptive grid techniques are subject to research for ship flows. They should bring considerable progress in accuracy without increasing computational effort excessively, but usually require unstructured grid capabilities of the code.

Numerical (non-physical) diffusion can be reduced by aligning grid lines along streamlines. However, flow separation and flow recirculation in ship flows allow this only to a limited extent.

Cartesian grids consist of elements with cell edges parallel to the axes of a Cartesian coordinate system. They are thus easy to generate, but unsuited for capturing complex geometries like ship hulls.

Therefore, in practice, generally *curvilinear grids* (body-fitted grids) are employed. These grids may be orthogonal or non-orthogonal. *Orthogonal grids* employ grid lines which intersect orthogonally. Since real ship geometries do not intersect the water surface orthogonally, at least some non-orthogonal grid lines have to be accepted. Otherwise, orthogonal grids are preferred since they facilitate the description of the discretized equations.

Curvilinear orthogonal grids require considerable effort in grid generation, but keep the complexity of the discretized equations relatively low. The velocity components may be grid oriented (local) or Cartesian (global). A formulation in Cartesian coordinates seems to react less sensitively to small deviations from smoothness in the grid.

Grid generation starts with specifying the cell faces on the boundaries (hull, water surface, inlet, outlet, outer boundary). Then the internal cell nodes are interpolated. Various techniques exist for this interpolation:

- *Algebraic grid generation* uses algebraic transformation and interpolation functions to create the grid geometry. For complex geometries (like real ship hulls), the resulting grid is often not smooth enough.
- *Conformal mapping* has been used for ships where the original mapping was enhanced by additional transformations to ensure that for real ship geometries the grids (within each two-dimensional section) were (nearly) orthogonal. However, this technique is fundamentally limited to two dimensions, i.e. for cross-sections. Smoothness and orthogonality in the longitudinal direction cannot be ensured automatically. Therefore, these grid generation techniques have been replaced largely by methods that solve a (simple) three-dimensional differential equation.

- *Grid generation based on differential equations* solves first a (relatively simple) differential equation subject to certain user-specified control functions or boundary conditions. The most popular choice is the Poisson equation, i.e. the Laplace equation with a specified non-zero function on the r.h.s. Thompson et al. (1985) describe such a method in detail which allows the user to control distance and orientation of the grid lines by specifying control functions. Poisson solvers create automatically smooth and orthogonal grids. Solving the Poisson equation can be interpreted physically as determining lines of constant temperature in the fluid where the ship is a heat source with heat distribution specified by the control functions.

Staggered grids specify, for example, the pressure at the cell center and the velocities at the cell faces. This improves automatically the numerical stability of the scheme, but is particularly unsuited for multigrid acceleration. Therefore staggered grids have become unpopular. Instead, other numerical techniques are employed to avoid pressure oscillations from cell to cell.

Grid generation is vital for the economic success of a CFD method. Grid techniques have been successively developed to allow more flexibility and faster grid generation:

- *Single-block structured grids.* Structured grids arrange cells in a simple $n_x \cdot n_y \cdot n_z$ array where each cross-section has the same number of cells, even though the cell shape and size may differ arbitrarily. Structured grids allow easy automation of grid generation and can easily be coupled with multigrid methods. They were traditionally employed because they allow simple program structures. Neighboring cells can be determined by a simple mathematical formula, avoiding the necessity for storing this information. However, this approach to grid generation does not allow the arrangement of additional cells in areas where the flow is changing rapidly. The choice is then either to accept insufficient accuracy in some areas or unnecessarily many cells (and thus computational effort) for areas where the flow is of little interest. In addition, complex ship geometries involving appendages are virtually impossible to model with such a grid. At least, the resulting grid is usually not smooth or involves highly skewed cells. As a result convergence problems are frequent.
- *Block-structured grids.* Block-structured grids combine various single-block grids. Each block is then structured and easily generated. But the block-structured approach allows some areas to discretize finer and others coarser. Blocks are also more easily adapted to local geometries, allowing smoother grids with largely block-like cells which improve convergence. The interpolation of results at each block requires some care, but techniques have been developed that allow accurate interpolation even for non-matching block interfaces, i.e. block interfaces where grid lines do not coincide. Block-structured grids are still the most popular choice in industry projects, typically involving 20—50 blocks for ship geometries.
- *Chimera grids.* Chimera was a fire-breathing (female) mythological monster that had a lion's head, a goat's body, and a serpent's tail. Chimera grids are arbitrarily assembled

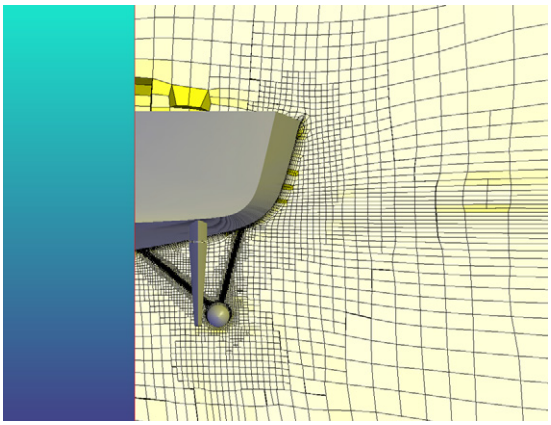

Figure 1.6:
Modern unstructured RANSE grid for ship with all appendages (one cross-section). *Source: NUMECA International.*

blocks of grids that overlap. They thus pose even fewer restrictions on grid generation and appear to be a very good choice for grid generation in ships, even though the interpolation between blocks is more complicated than for block-structured grids.

- *Unstructured grids.* Unstructured grids allow the largest flexibility in grid generation (Fig. 1.6), but require more effort. Unstructured grid programs can also handle structured or block-structured grids. One may then generate a simple grid and use adaptive grid techniques which automatically generate unstructured grids in the computation. Unstructured grids are popular, e.g. for aerodynamic flow analyses around superstructures of ships. Here the complexity of the boundary geometry makes other grid generation approaches at least very tedious. Adaptive grids and formal optimization procedures (requiring fully automated grid generation) are trends that will make unstructured grids the long-term preferred choice in many practical applications.